Bollettino di Geofisica Teorica ed Applicata Vol. 55, n. 2, pp. 369-387; June 2014
DOI 10.4430/bgta0123

Reflection seismic images from OBS profiling across External Hellenides

E. Barison, R. Nicolich and G. Brancatelli

Department of Civil and Environmental Engineering, University of Trieste, Italy

(Received: January 11, 2011; accepted: July 9, 2013)

ABSTRACT Seismic profiles were planned and acquired on the western offshore continental margin of Peloponnese within the framework of the EU-SEAHELLARC project. A large number Ocean Bottom Seismographs (OBSs) recorded shots from an airgun source on board of the R/V OGS-Explora and HCMR-Aegaeo for deep crustal prospecting. They were deployed in deep water and a rough sea bottom topography and lined up with four profiles. The technique was proposed to partially substitute a deep seismic reflection survey with a long streamer and large airgun sources. The processing of these data as standard reflection seismic data was performed utilizing only near vertical incidence after relocation of OBSs at the sea-surface. At the beginning we picked the first arrivals for a tomographic inversion to create a detailed near sea bottom velocity model by iterative ray-tracing and travel time calculations. The information was used to relocate shots and OBSs (receivers) to the same datum plane applying the Wave Equation Datuming (WED) and subsequently for dynamic corrections, migration and depth conversion. WED, operating on a common-source gathers, has the effect of extrapolating the receivers from one datum to another, and, because of reciprocity, operating on a common-receiver gather, changes the datum of the source. The WED process of upward or downward continuation of the wave-field between two arbitrarily shaped surfaces requires the datum surface totally below or above the sea bottom morphology. We utilized an intermediate datum plane first, at 5 to 6 km depth (downward continuation), then OBSs and shots were relocated to the sea surface (upward continuation). The intermediate depth datum solution is required to bypass near sea bottom tectonic complexities and to increase the number of traces (along the profiles there are more shots and closer to each other than OBSs), which contribute to Kirchhoff summation in the migration procedure. WED removed time shifts related to the water layer and to near sea bottom tectonic complexities and velocity variations. A conventional processing sequence was then applied to the corrected data obtaining images of the deep crustal interfaces with an upper and a lower plate separated by an intra-plate detachment reflecting interval at 10 to 20 km depth on the different profiles. The Moho seems to be gently dipping from north to south and from the Ionian Sea towards the Peloponnese to where the collision of the Ionian cold and brittle crust with the Hellenic crustal roots was recognized with a pronounced crustal flexure reaching depths of more than 35 km beneath the western Peloponnese coasts.

Key words: wave equation datuming, static corrections, ocean bottom seismometers, crustal structures, Peloponnese continental margin, SEAHELLARC.

1. Introduction

The area under investigation is located on the External Peloponnese continental margin, a segment facing the deep Ionian basin and part of the western border of the Hellenic subduction zone (Fig. 1).

A detailed submarine morphological-geological background of the margin area was one objective of the European SEAHELLARC project (see Papoulia *et al.*, 2014), completed with the reprocessed data of Multichannel Reflection Seismic (MCS) profiles recorded in the 1980s

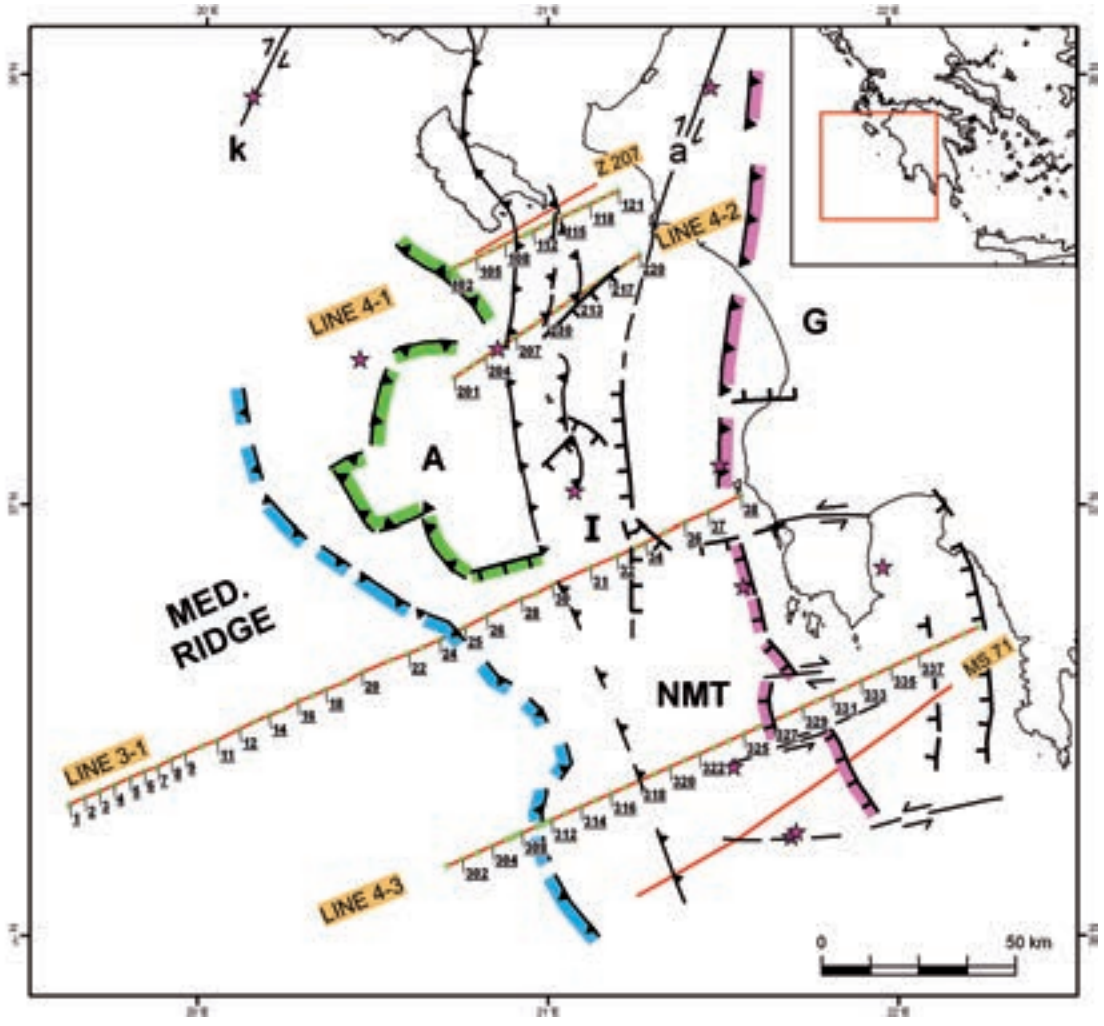

Fig. 1 - The surveyed area with the position of the OBSs annotated on the different profiles (Lines 4-1, 4-2, 3-1, 4-3). The oversimplified subdivision of the tectono-stratigraphic zones (G = Gavrovo; I = Ionian; A = Apulia) was derived from the interpretation of the MCS profiling [red tracks in the map for the profiles Z207 and MS71: see Wardell *et al.* (2014)]. The buried and dissected deformation front of the Gavrovo G-zone (pink) and of the Ionian thrust I-zone (black) over the Apulian Ridge (A) and the Apulian Ridge frontal thrust (green) are indicated, together with the backthrust of the Mediterranean Ridge complex (blue) (from Chamot-Rooke *et al.*, 2005). The Cephalonia (k) and Andravida (a) dextral strike-slip faults (see text) and the region of the NMT are displayed . The pink stars point to the epicentres of the more characteristic earthquakes of the area (Slejko *et al.*, 2014).

by the National Hellenic Oil Company and by Istituto Nazionale di Oceanografia e di Geofisica Sperimentale (OGS) (Trieste, Italy) in the 1970s (Wardell *et al.*, 2014). All the data were used to locate active faulting potentially able to generate important ruptures and subsequent onshore catastrophic events (earthquakes and tsunamis).

Additionally an onshore/offshore seismic array with ocean bottom seismographs (OBSs) was established and an active and passive seismic study was performed in order to build a velocity model for the crustal structures and define the seismogenic zones more accurately. Four profiles, with a large number of deployed recording instruments and shooting airguns from the ships, were planned to obtain wide-angle structural models of the crust of External Hellenides area. This technique was proposed to partially substitute a deep seismic reflection survey with a ship equipped with a long streamer and large airgun sources that was not available at that time.

The extremely complex local geologic structures with the presence near the irregular sea bottom of hard rocky formations with high velocity such as carbonates or salt intrusions, alternate with recent marine soft deposits, and the low energy of the airgun source installed on the ships, made it difficult to uniquely identify and correlate the wide-angle refraction/reflection phases from OBS to OBS along each profile. To resolve this difficulty in intepretation, the idea was to process the profiles, with a relatively narrow OBS spacing, as a standard near vertical incidence reflection seismic data set, trying to evidence images of deep crustal interfaces and to extend downwards the interpretation of the MCS sections which only penetrated the first 5 - 6 km of the upper crust.

To organize the reflected seismic signals with a common datum plane for shots and receivers (the OBSs), the usual static corrections are not verified and complex methods, such as the Wave Equation Datuming (WED), were used for our acquisition with large offsets and large elevation differences in shot-receivers positions. WED contributed also to remove time shifts related to near sea bottom tectonic complexities and velocity variations, to enhance higher frequencies, increase resolution and improve signal/noise ratio.

Fig. 1 shows the position map of the OBS profiles together with the tracks of the two MCS profiles cited in the text and with a few indications of the principal structures characterizing the prospected tectono-stratigraphic zones.

2. Geologic setting

The surveyed domain was originally part of the passive continental margin of Africa (Apulian) plate with Mesozoic carbonates occupying a wide zone from the Adriatic Sea to the eastern Cretan area. It was extended by rifting from Early-Middle Jurassic with the formation of large oceanic areas and of structural highs followed by depressions, both filled later by shallow water carbonates on the ridges and by pelagic sequences in the basins. It is now part of the foreland with westward directed folds and thrusts typifying the External Hellenides, the upper plate that overrides the ocean-floored Ionian basin lower plate subducting eastwards (Kamberis *et al.*, 2000; Sotiropoulos *et al.*, 2003; Van Hinsbergen *et al.*, 2006). The thrusts have developed since Early Cretaceous resulting from the collision of the Apulian microplate with Eurasia after the closure of the Tethys ocean [see e.g., the geodynamic reconstructions of Jolivet and Brun (2010)].

A detailed description of the tectonostratigraphic zones characterizing the External Hellenides is presented in Wardell *et al.* (2014). Fig. 1 shows the position of the deformation front of the

strong and rigid platform carbonates with their metamorphic basement of the Gavrovo zone, recognized on land in outcrops in the western Peloponnese (Kamberis *et al.*, 2000) but buried at sea. Some tectonic structures featuring the Ionian zone and the position of the front of its thrusts over the Apulian Ridge zone are indicated in the same figure. The Ionian zone is primarily characterized by the presence of pelagic carbonates with complex structural deformations including Triassic salt intrusions and diapiric movements also upsetting the near sea bottom sedimentary cover in the basins. Active extensional tectonics are recognized in the reactivation as normal faults of the thrusts, and also transfer faults, accompanying the westward movements of the deformation fronts, are identified. This background is controlled by the general SW-ward anticlockwise movements along the main dextral strike-slip faults (Papanikolaou and Royden, 2007; Wardell *et al.*, 2014).

The backthrust front of the Mediterranean Ridge complex (Chamot-Rooke *et al.*, 2005), the Cephalonia (k) dextral strike-slip fault (Sachpazi *et al.*, 2000) and the southward extension of the parent Andravida or Achaia-Elia fault (Feng *et al.*, 2010) are also indicated in Fig. 1, as well as the position of the North Matapan Trough (NMT), part of the Inner Plateau and basins of the Mediterranean Ridge, the western actively deforming accretionary pile resting over a continental backstop of variable width (Truffert *et al.*, 1993; Le Pichon *et al.*, 2002).

3. OBS profiles

3.1. The OBS data acquisition

The OBSs (manufacturer GeoPro GMBH, Hamburg) were equipped with 4 recording channels (three geophones with natural frequency of 4.5 Hz and one hydrophone) and deployed in water depths from a few hundred metres to more than 4600 m. The source was an array of 16 airguns with a total volume of 39.4 litres (39.4 x 10^{-3} m^3), fired at a depth of 9 m from the research vessels Aegaeo (recording Line 3-1) and OGS-Explora (Lines 4-1 to 4-3). The shot time-interval was 60 s, corresponding to about 120 m (Table 1). The data were sampled at 4 ms and the length of the processed records was 20 s.

Table 1 - Summary of the main acquisition data.

Lines	Total Length (km)	N° of OBS	OBSs average distance (km)	Total shots	average shot interval (m)
Line 4-1	60	20	2.7	528	115
Line 4-2	72	19	3.2	634	123
Line 3-1	192	28	5.0	1586	120
Line 4-3	162	30	4.2	1315	124

3.2. OBS data processing

OBS recordings are usually processed as wide-angle reflection/refraction data with a forward modelling and iterative travel-time inversion in order to obtain velocities and depth positions of the crustal interfaces.

Our aim was to use refracted first arrivals to build a reasonable velocity model for the upper sequences of the sedimentary crust where significant complexities in the structural setting with variable lithologies and velocities are present. The algorithm is based on the minimization of differences among calculated and observed travel times with offsets ranging from 3 to about 40 km. This corresponds to the maximum distance with clear useful first-arrival energy for the application of refraction tomography evaluation of the shallow layers, with data redundancy and an adequate signal to noise (S/N) ratio. The total numbers of picks was 20,143. Pre-processing was applied to increase the signal to noise ratio with amplitude recovery and balancing to homogenize the shot and receiver responses. Trace editing to remove the noisier parts of the signal, a bandpass filter, spike deconvolution, linear move-out with a reduction velocity of 6 km/s completed pre-processing.

The commercial software VISTA® (GEDCO-Schlumberger: www.gedco.com) was used for the data pre-processing and TomoPlus® (GeoTomo LLC: www. geotomo.com) for the definition of the velocity table from refracted first arrival tomographic inversion.

In the tomographic inversion, we defined 65 m wide square cells corresponding to the half-shot distance. Forward ray-trace modelling was carried out in order to obtain a reliable initial model attaining the final representation after 25 iterations. The bathymetry was included in the ray tracing and the water velocity was considered constant and equal to 1500 m/s. The first output was re-entered in the tomography process as a new initial model, and submitted again to 25 iterations before attaining the final result.

Fig. 2 shows an example of a warped first arrival pattern by a rough sea bottom topography and highly variable rock velocities; Fig. 3 shows the observed (picked) and computed travel times for the Line 4-3.

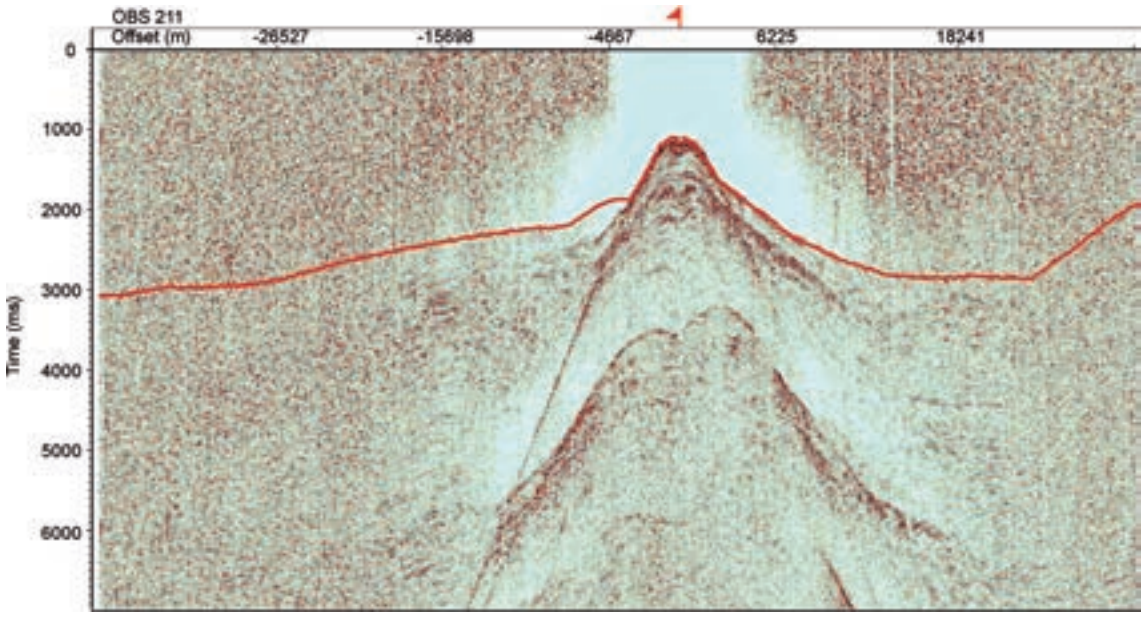

Fig. 2 - One OBS record section (OBS position nr. 211 on the Line 4-2) with the first arrivals pattern (in red) controlled by the rough sea bottom topography and by strong velocities variations. The S/N ratio is unfavourable.

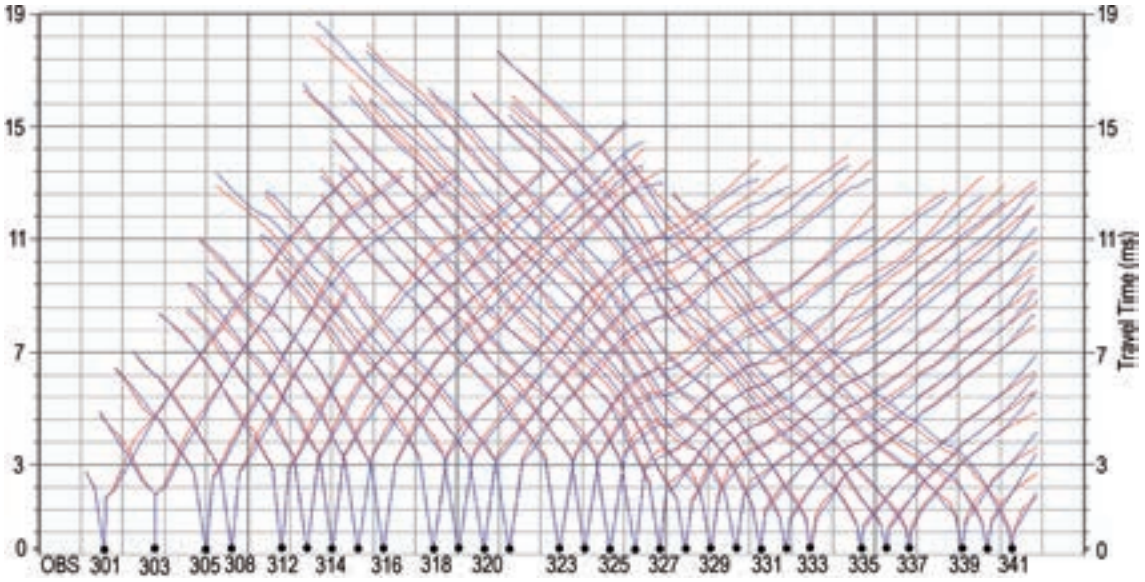

Fig. 3 - An example of observed and computed travel times from first arrival picks for the Line 4-3 (position in Fig. 1).

The maximum investigated depth with reliable velocity values ranged from 3 to 5 km beneath the sea bottom, corresponding to the better resolved sectors covered by an adequate number of forward and reverse travel times. An example is given in the model of Fig. 4 where the near surface velocity distribution for the Line 4-1 recalls the images of the section from the nearby multichannel profile Z207 (from Wardell *et al*., 2014). The wide Ionian zone flexure, filled by a thick flysch unit originated from the erosion of internal formations and by recent marine deposits, is evidenced by the lower velocity intervals (from 2000 to 4000 m/s) facing the ridge. Here the frontal thrust of the Ionian zone over the Apulian Ridge zone is detected.

The velocity models computed for each profile contributed to the construction of the seismic image of the deep crust from the processed OBS data with post-stack depth migration after the relocation of OBSs to the sea surface. Shots and receivers are normally relocated at a given datum level by static corrections that remove the time shifts caused by velocity changes in the shallow layers. The assumption of a vertical near-surface raypath is adopted when static corrections are applied. This hypothesis is adequate when: i) the static time shifts are small; ii) the top layer has a velocity considerably lower than all following layers. However, these assumptions are not verified for acquisitions with large offsets in shot-receivers positions with considerable emergence angles where the hypothesis of vertical ray paths is not consistent with wavefield propagation (Bevc, 1997) or with significant lateral velocity variations near the surface, such as OBSs deployed in deep waters and rough sea bottom topography (Fruehn *et al*., 2001). In these cases more complex methods, such as the WED, should be used.

In the pre-stack domain, WED is applied in two steps: i) common-source and ii) common-receiver domains. The operation on a common-source gathers extrapolates receivers from one datum to another, and, because of reciprocity, operating on common-receivers gathers, changes the datum of the source. The Kirchhoff integral solution to the scalar wave equation (using both near-field and far-field terms (Berryhill, 1979, 1984) can provide a basic computation to deal with

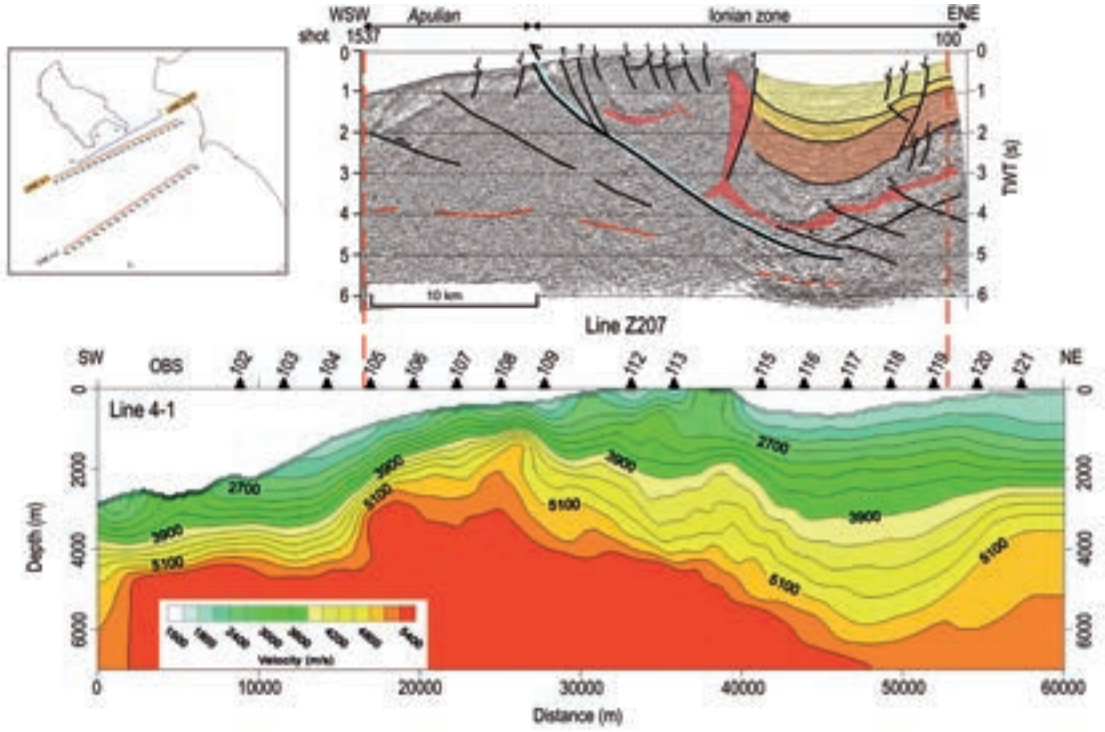

Fig. 4 - The velocity distribution to 6 km depth from tomographic solution for Line 4-1 compared to the interpreted section of the nearby multichannel reflection seismic time-migrated profile Z207 (after Wardell *et al.*, 2014). The image of the velocity pattern fits the suggested structures and lithologies of Ionian and Apulian zone with carbonates thrusts and Triassic salt (red) against piggy-back deposits with flysches (brown) and recent sedimentation (jellow).

irregular surfaces (Wiggins, 1984) and variable velocities.

It is important to distinguish between migration and WED (i.e., Barison *et al.*, 2011). Migration involves computing the wavefield at all depths from the wavefield at the surface, i.e., it can be intuitively explained as a succession of downward continuation steps, with the elevation z moving ever deeper into the subsurface. In addition to downward continuation, migration requires imaging principles (Yilmaz, 2001). WED produces an unmigrated time section at a specified datum plane. In this respect, WED is an ingredient of migration, when migration is done as a downward-continuation process. Basically, WED is the process of upward or downward continuation of the wave field between two arbitrarily shaped surfaces. The method was generalized by Berryhill (1984) to pre-stack data by applying the same extrapolation algorithm to common-source gathers and, finally, to common-receiver gathers. The velocity used in extrapolation is that of the medium confined between the input and the output datum. More details have been added in the Appendix and in the paper of Barison *et al.* (2011).

The Seismic Unix (SU) package, a free software developed at the Colorado School of Mines, was utilized to carry out WED and the final migration. The code [written by Salinas and based on Liu (1993)] uses a far field approximation of the Berryhill (1979) original formula. This application requires a regular geometry and zero traces must be carefully introduced to have a regular distance between receivers and shots in each common shot and common receiver gather.

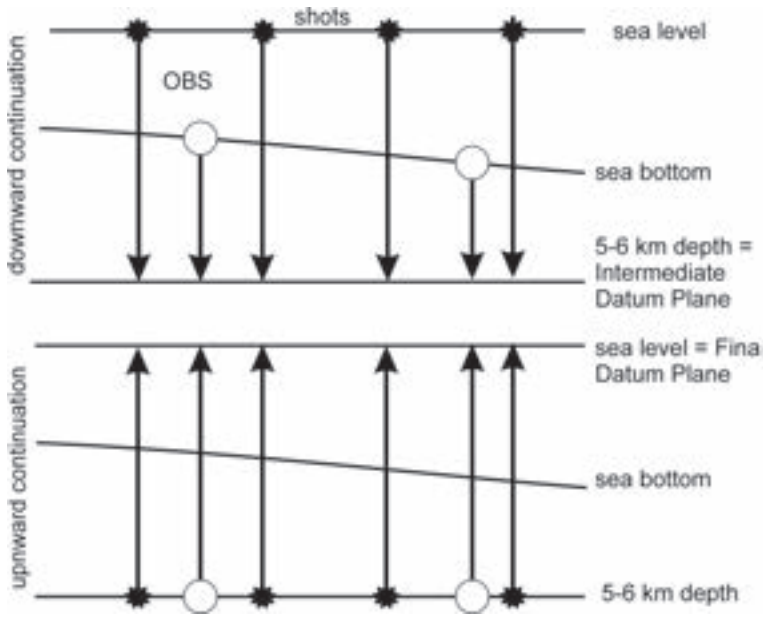

Fig. 5 - Schematic representation of the downward continuation procedure of the data to a flat intermediate depth datum plane and of the upward continuation with the relocation of shots and receivers to the sea surface.

We moved the OBSs (receivers) and shots to an intermediate datum plane first, at about 5-6 km depth below the sea level (downward continuation), and then the OBSs and shots were relocated to the sea surface, the final datum plane (upward continuation). The intermediate depth datum solution (Fig. 5) is required to increase the number of traces (along the profiles there are more shots and closer to each other than OBSs), which contribute to Kirchhoff summation in the migration procedure, considering the OBSs as source points and the shots as receivers. It was not possible to find a continuous reflecting marker as an intermediate datum because of the complex thrust tectonics affecting the area and the poor S/N ratio. The depth was settled below the near sea-bottom heterogeneous structures and where the seismic velocity appears to be definitely higher than 5.0-5.5 km/s. Our choice means that a partial migration was applied two times gaining a further reduction of the amplitudes of anomalous events and noise, with the preservation of the velocity information for the depth converted sections. Moreover, it is important to underline that WED suffers from spatial aliasing, because it is based on a wave extrapolation process and the OBS acquisition requires verification of the possible aliasing. First of all, we evaluated the Fresnel zone and found a Fresnel radius equal to 1095 m [assuming a velocity of 4000 m/s at 6 s two ways travel time and a dominant frequency of 20 Hz: Yilmaz (2001)]. This radius is much larger that our traces distance (about 120 m). The amplitude spectra in Fig. 6, before and after WED application, show that no spatial aliasing is present, as expected. WED enhanced higher frequencies and the amplitude spectrum becomes roughly flat, thus increasing resolution.

The downward continuation of the velocity field from the tomographic solution, to be used in the successive processing steps, was obtained by velocity extrapolation to depths of 25-35 km (an example in Fig. 7). A vertical and horizontal smoothing was applied to a positive velocity gradient to avoid artefacts such as velocity pull-up or down in the depth sections. The velocity distribution at depth in the models is compatible to the information derived from the

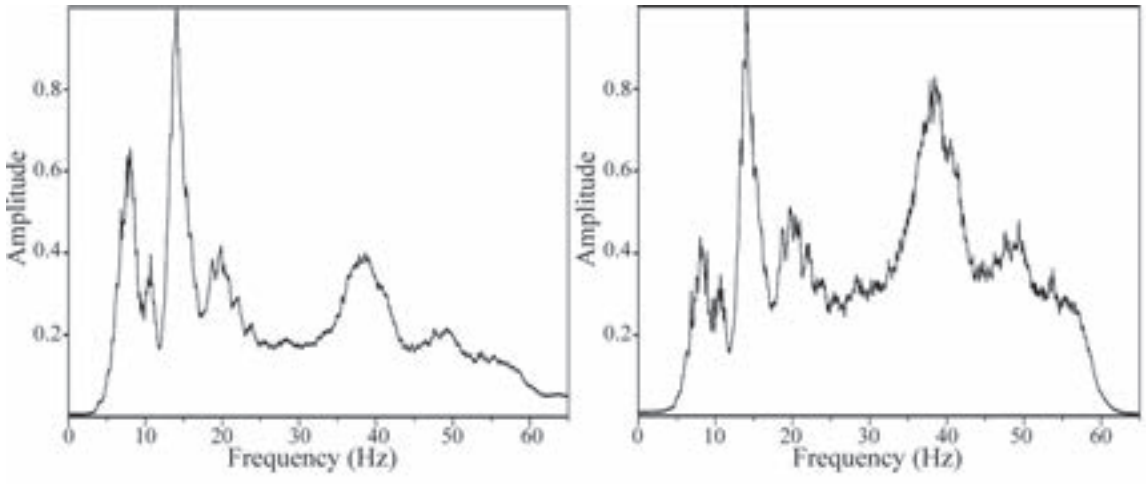

Fig. 6 - Amplitude spectrum of an OBS record before (left) and after (right) WED. OBS signals are normalized to the maximum amplitude. The higher frequencies are enhanced and the spectrum is flattened, after WED.

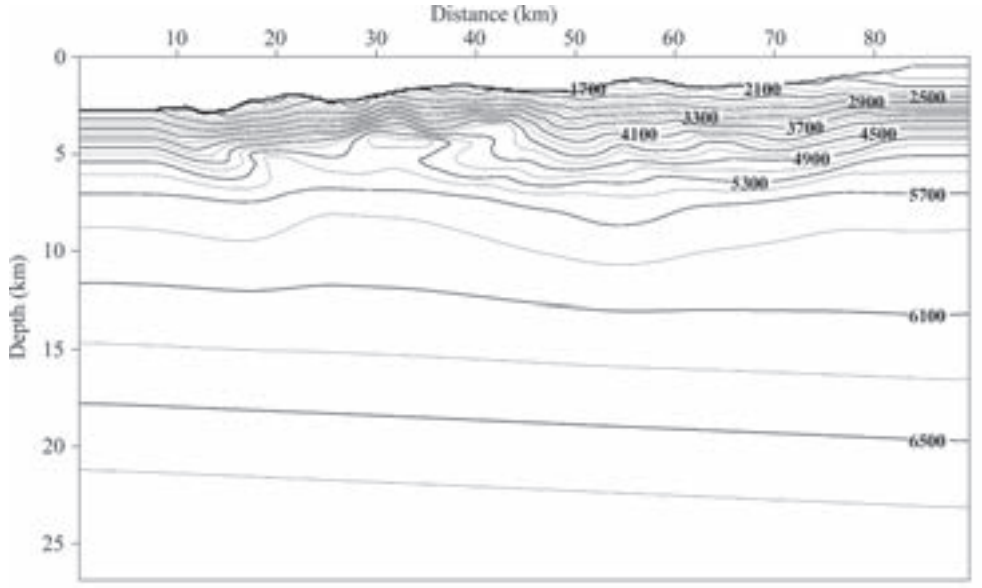

Fig. 7 - An example of the velocity distribution as obtained from first breaks tomographic inversion for the Line 4-2. The velocity field has been extended downward to the crustal depths for dynamic corrections and migration, considering a gradual positive variation. The well defined near sea-bottom velocities are recalling the reflection images of the composite section from MCS profiles KY301, Z151A, Z151B (Wardell *et al*., 2014).

processing of MCS profiles and the interpretation of wide-angle profiles acquired in the Ionian Sea (Makris, 1978; Truffert *et al*., 1993; Clément *et al*., 2000; Fruehn *et al*., 2002; Jones *et al*., 2002). In the end, we converted the computed interval velocities into a rms-velocity table for WED application, NMO corrections, stack, migration and depth conversion. Errors in the depth conversion values may derive from a non-precise downward extrapolation of the velocity functions.

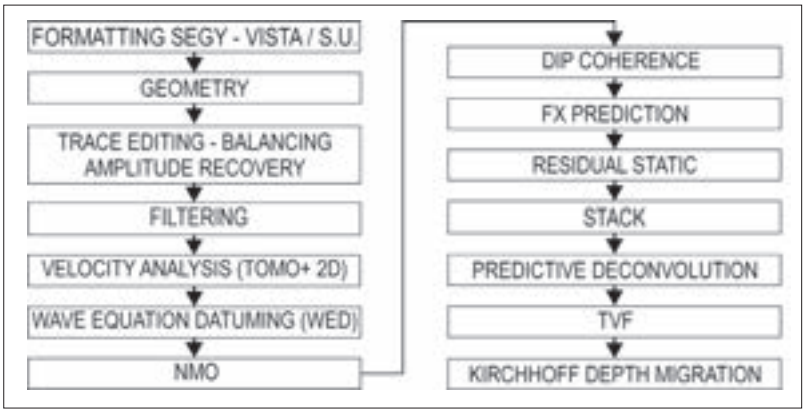

Fig. 8 - Processing flow-chart.

The successive processing steps (the flow chart in Fig. 8) included deconvolution and 2D filtering to enhance the lateral continuity of the reflections and to remove coherent noise, and a time variant filter to improve the imaging of the stack section. Finally, a post-stack Kirchhoff depth migration was applied.

3.3. Results and interpreted seismic sections

The OBS profiles were processed to emphasize the geological and geophysical significance of the seismic images of the crust. The poor S/N ratio, the low energy of the source with reduced wave penetration, the limited or missing coverage of the shallow layers and the complex tectonic setting do not always give clear reflection images of the geological units.

The depth section for the OBS Line 4-1 is shown in Fig. 9. The interpretation is limited to some white and transparent, thick lines, to indicate east-dipping markers in the upper part followed by a planar or gently dipping reflective system in the lower sectors.

The upper thrusts of the Ionian and Apulian Ridge nappes, with east-dipping reflecting markers, are poorly resolved because of the muting of non near-vertical incidence events and the obvious lack of coverage, but they are separated from the underneath lower plate by sub-horizontal layers. The lower plate is delineated below by an interface near the bottom of the reflective layerings, which generally are considered in reflection seismic to correspond to the base of the crust: the Moho (M) at depths from about 20 (SW) to 21 km (NE). The intra-plate reflective marker (I in Fig. 9) is indicated at around 11 km depth (SW corner) gently down dipping NE-wards. It denotes the position of the interval separating the upper from the lower plate.

The depth section for the OBS Line 4-2 (Fig. 10) has a similar character to the previous one, but with a low S/N ratio where greater tectonic complexities exist. The proposed depths of the two main interfaces, I and M, are slightly increased moving southwards: approximately 11 to 14 km for the intra-plate, 21 to 24 km depths for the Moho.

Similar interfaces are found in the data published by Clément *et al*. (2000) and acquired in the area among Cephalonia, Zakynthos and the Kyparissiakos Gulf with MCS and wide-angle prospecting utilizing an airgun source operating in single-bubble mode. The wide-angle reflected/refracted signals were acquired by a land station, shooting at sea. The above authors

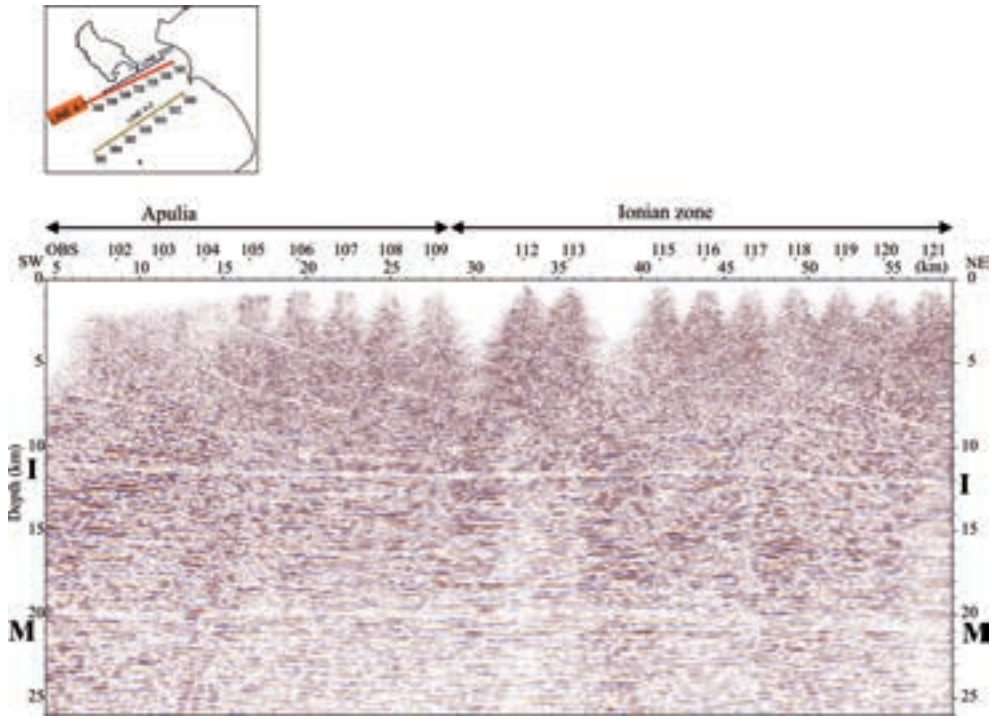

Fig. 9 - Depth section for the OBS Line 4-1. The sketched interpretation identifies the western-directed Hellenic nappes of the upper plate where migration smiles from low coverage interfere with dipping reflectors. I (intra-plate interface) separates the upper plate with eastward dipping layering from almost flat reflectivity of the lower plate; M (Moho) corresponds to the termination of the high reflectivity of the lower plate interval.

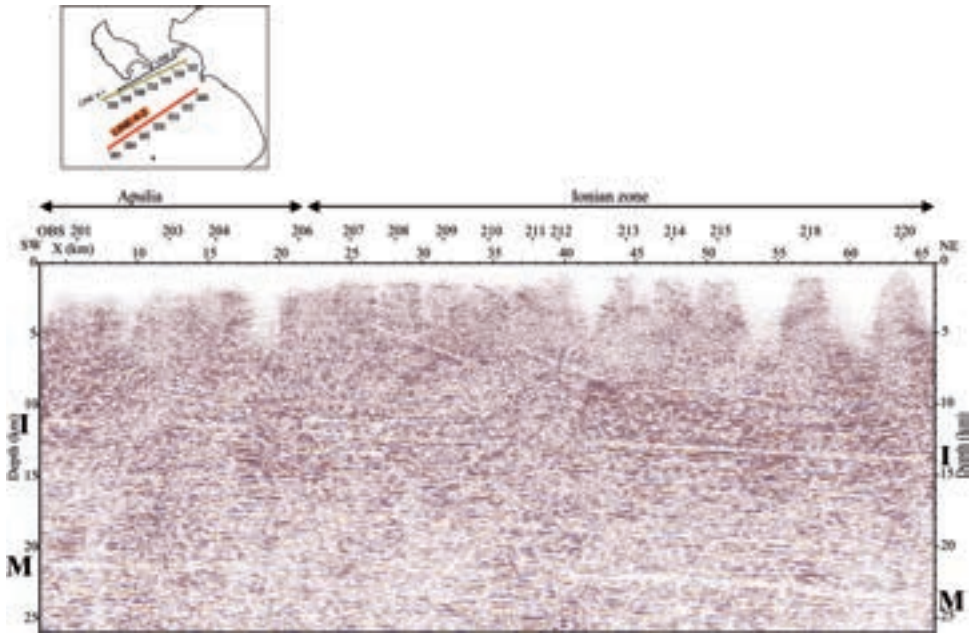

Fig. 10 - Depth section for the OBS Line 4-2: I = intra-plate interface; M = Moho, at the base of the lower plate. The structural setting seems difficult to depict with very noisy data.

proposed a Moho at 20 to 22 km depth gently dipping eastwards. Controlling depth and velocity of the water layer, substituted by that of the sub-bottom thrust folds of carbonates, they avoided velocity artifacts in MCS profiling and confirmed the inter-plate layer at 7 to 9 s reflecting times, dipping eastwards. This interface was considered to indicate the base of the upper plate thrusts and was proposed at a depth of 12 to 14 km. A similar marker was found by Him *et al*. (1996) at comparable depths, north of Zakynthos. Those authors reached the conclusion that Apulian Ridge and Ionian zones overrode the ocean-floored Ionian Sea lower plate during late Neogene according to Underhill (1989).

Investigations on crustal structures of the area by wide-angle profiling were promoted by Makris (1978), who defined the Moho depth at around 20 to 26 km from the eastern Ionian Sea to the western Peloponnese coast-line. From there, in 10 km, the crustal thickness becomes of more than 40 km beneath the central-western Peloponnese (the position of the Hellenides crustal roots).

Suckale *et al*. (2009) revealed the subduction of the oceanic Ionian crust by the computation of high resolution receiver functions. They positioned the top of the slab at about 35 km beneath the western Peloponnese coasts, reaching depths of 150 km in correspondence of the eastern coasts. Gesret *et al*. (2010) confirmed the oceanic nature of the African slab subducted under Peloponnese.

The data acquired along the OBS Line 3-1 are in general poor and not all usable in the stack section, with reduced coverage due to missing records. The depth section of the south-western part of the long profile (Mediterranean Ridge area) is shown in Fig. 11 with the intra-plate

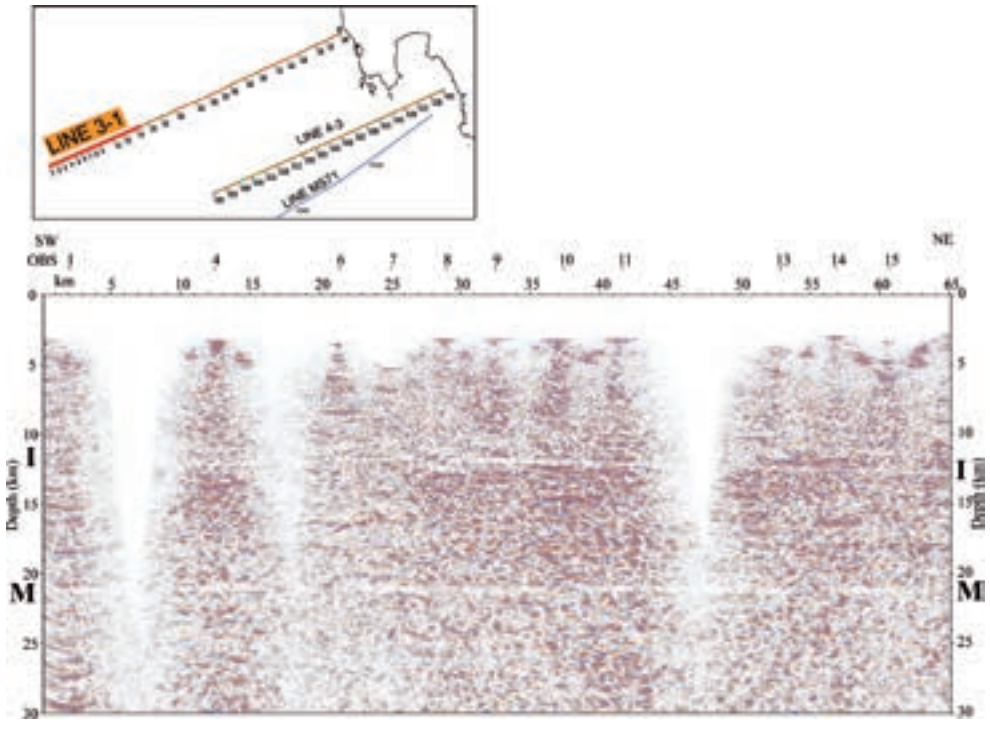

Fig. 11 - Depth section for the south-western sector of the Line 3-1 crossing the Mediterranean Ridge: I = intra-plate interface; M = Moho, at the base of the lower plate. Some spot images among missed records are well connoting our interpretation of the two interfaces.

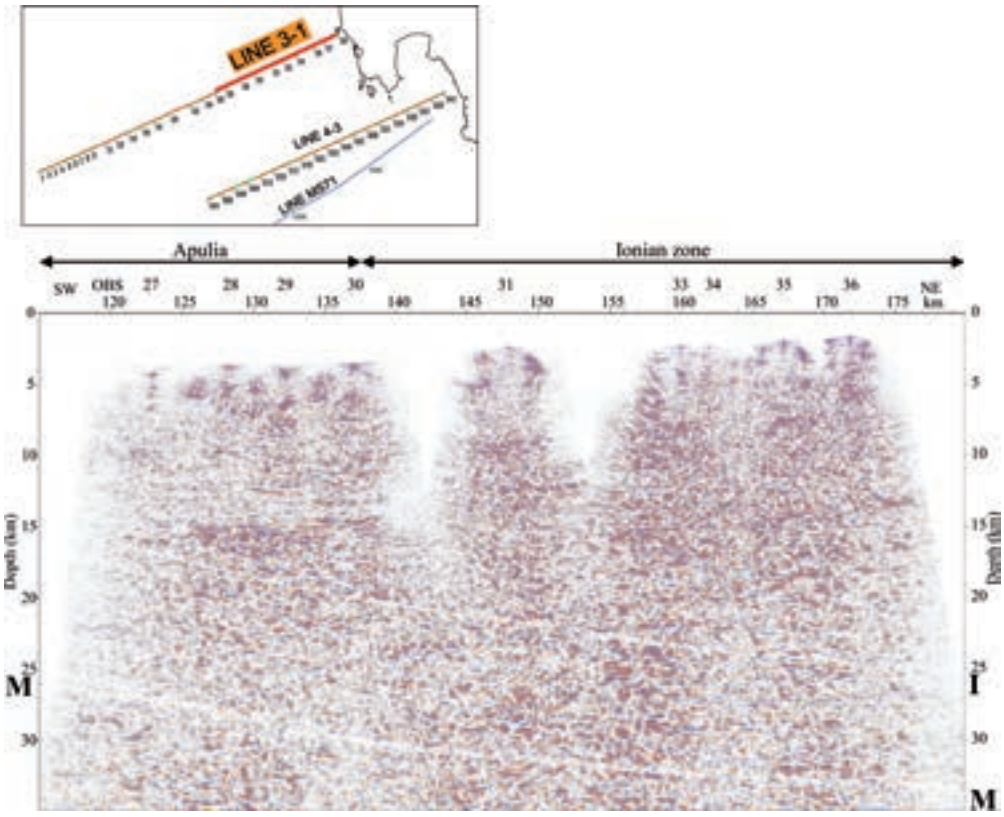

Fig. 12 - Depth section for the north-eastern sector of the Line 3-1: I = intra-plate interface; M = Moho, at the base of the lower plate next to the collision with the thickened Hellenic crust. Our interpretation considers a lower plate down-bended from about 26 to 35 km or more.

detachment layer around 12-13 km depth and the Moho at about 21 km depth. These reflectors are well recognized by some intermittent reflections and by the termination of the corresponding layerings. The easternmost part of the Line 3-1 is presented in Fig. 12, where we observe the collision of the Ionian basin lower plate with the thickened Hellenic crust in concurrence with the position of the Gavrovo zone deformation front (see the tectonic scheme in Fig. 1). We propose for this intricate image an interpretation, which considers the presence of a large slice of the Hellenic crust with Gavrovo shelf limestones and metamorphic-crystalline units over the thin Ionian Sea cold and brittle crustal unit, rapidly flexured downwards from about 26 to 35 km or more, in continuity also with the observations of Suckale *et al*. (2009) in the Peloponnese Peninsula.

The southernmost OBS Line 4-3 is crossing the NMT. The velocity field, presented in Fig. 13, highlights the Gavrovo high velocity units to the east in contrast to the low velocities for the sediments filling the trough. In Fig. 14 the depth section of the north-eastern part of the profile. The intra-plate marker is proposed around 16 km depth at the south-western corner, dipping eastwards and reaching apparently 20 km depth in correspondence of the OBS position 327. The lower plate shows a thickness of approximately 9 km with the Moho at 27 km (to the west) reaching approximately 37 km at the eastern end of the profile. The pronounced flexure

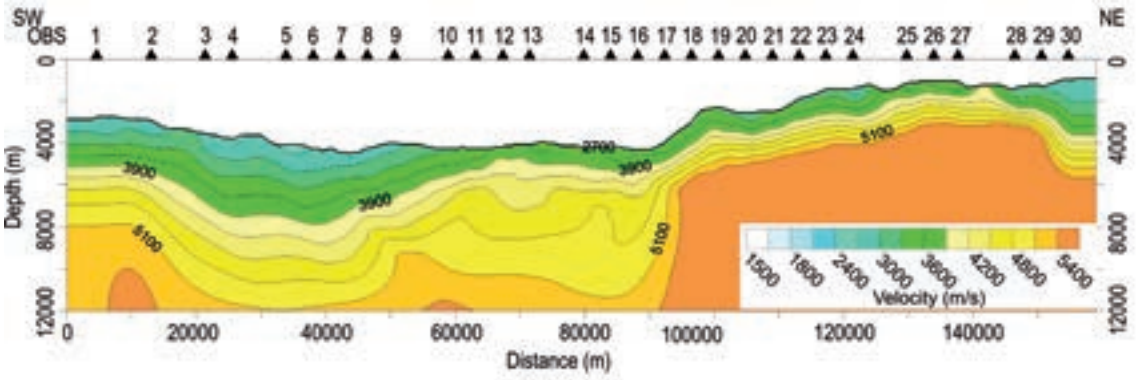

Fig. 13 - Results of the tomography solution along the Line 4-3 with the Gavrovo high velocity units to the east in contrast to the low velocities for the sedimentary units in the NMT.

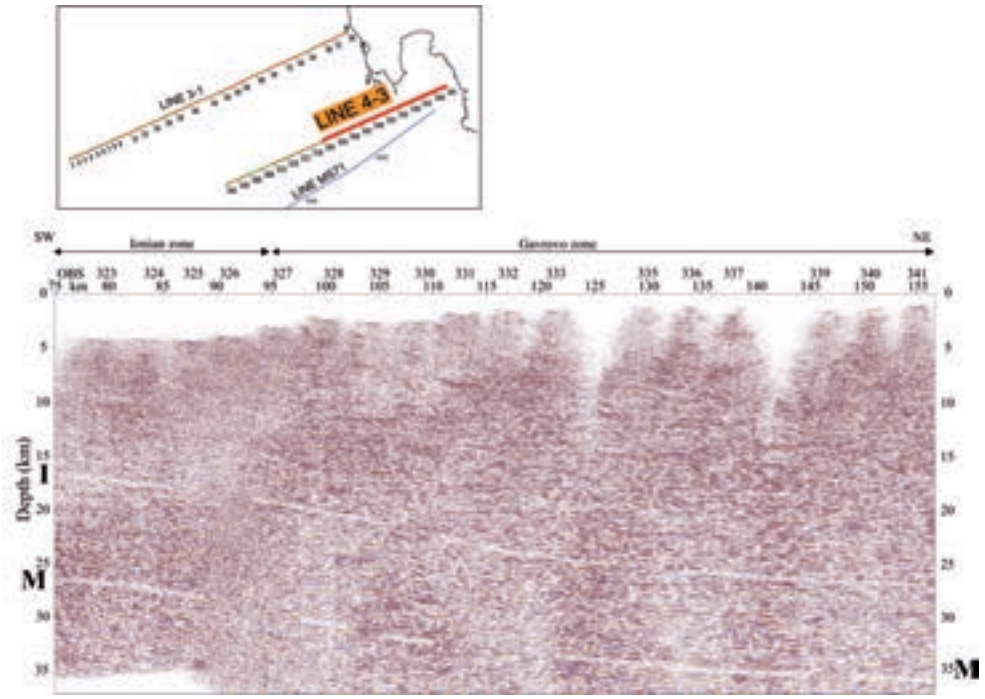

Fig. 14 - Depth section for the north-eastern sector of the Line 4-3: I = intra-plate interface; M = Moho, at the base of the lower plate. The interpretation scheme repeats that of the Line 3-1.

of the lower plate is recognized to begin at the collision of the Ionian with the Hellenic crust. The Gavrovo zone shelf sequences with their basement is revealed by the high velocity obtained from the tomographic inversion (Fig. 13).

The important changes in the structural setting in correspondence of the OBS position 327 can be seen also in the sketched interpretation (Fig. 15) of the nearby multichannel profile MS-71 (position in Fig. 1), reproduced from Wardell *et al.* (2014). The NMT appears not to be a subduction trench, but it may instead represent a piggy back thrust propagating system shaped by a presently active extending half-graben (Lallemant *et al.*, 1994; Laigle *et al.*, 2002). The

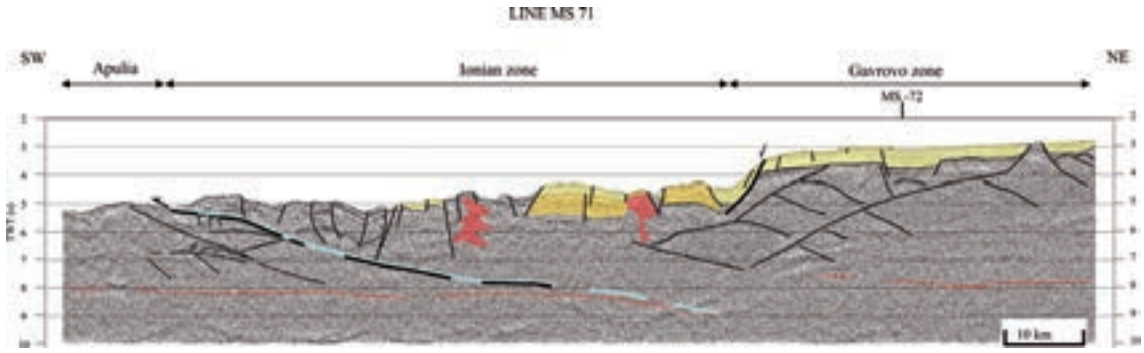

Fig. 15 - Sketched interpretation of the MS-71 seismic profile showing the thrusts of Gavrovo zone shelf limestone the corresponding metamorphic and crystalline basement over the Ionian zone basinal sequences with plastic flysches filling the flexure (a piggy back thrust propagating system). The Gabrovo frontal thrust has been reactivated as normal listric faults. The deepest reflector (in red) may correspond to the intra-plate layer separating the upper and lower plate.

profile shows the reactivation of the easternmost Hellenic thrust fronts with very impressive normal faults highlighting the present-day extensions dominating the upper plate.

4. Conclusions

We applied WED approach to OBS acquisitions for deep crustal prospecting. The project did not initially include the use of OBSs in the reflection seismic profiling but we attempted to resolve problems of signal recognition in an adverse geologic setting. We considered only the vertical component in the OBS, unable to utilize, because of poor S/N ratio, the other two horizontal channels. Also the noisy pressure data from the hydrophones did not allow us to make use of them, for example for amplitude reduction of water bottom multiples. First order water bottom multiples were enhanced adding noise and hindering the identification of the primary horizons. The depth sections corresponding to the OBS profiles give some hints of the crustal structures with the separation of an upper and a lower plate by an intra-plate detachment interval at a depth of around 11 km (in the northernmost profile) to about 20 km (in the southernmost one). The depths increase moving from north to south and from west to east and remain well defined in the upper part where velocities have been constrained by tomographic inversion, but uncertainties could influence the position of deeper interfaces because of the extrapolation procedure used to construct the velocity field for depth conversion. The presented interpretation of crustal sections are consistent with previous cited researches in the region, including the model of the Mediterranean Ridge, presented by Fruehn *et al*. (2002) and derived from IMERSE-OBC and MCS data, where the intra-plate detachment interface was also outlined.

The stack of the External Hellenides nappes is inaccurately imaged in the upper plate because of the low coverage after muting of noisy traces. The Ionian basin crust, with sub-parallel layers down to the Moho, presents a thickness of around 9-10 km and is gently dipping from north to south and from the Ionian Sea basin towards the Peloponnese coasts. Near the coast and near the buried frontal thrust of the Gavrovo tectono-stratigraphic zone the seismic images become

intricate because of the poor S/N ratio. Our interpretation suggests a downward flexure of the Ionian cold and brittle oceanic crust where it collides with the thickened Hellenic continental one and where the base of the Ionian crust is thought to quickly reach depths close to 35 km. In this context the upper plate appears to be actively overriding the subducting lower one behaving rather like to a passive plate margin.

Acknowledgements. The OBS data were acquired within the project SEAHELLARC (EU-037004) with the participation of the partners: GeoPro-Hamburg; HCMR-Athens and OGS-Trieste. U. Tinivella, M. Giustiniani and F. Accaino are acknowledged for their contribute in the OBS-WED processing, and N. Wardell for the improvements given to the manuscript.

REFERENCES

Barison E., Brancatelli G., Nicolich R., Accaino F., Giustiniani M. and Tinivella U.; 2011: *Wave equation datuming applied to marine OBS data and to land high resolution seismic profiling*. J. Appl. Geophys., **73**, 267-277.

Berryhill J.R.; 1979: *Wave-equation datuming*. Geophys., **44**, 1329-1344.

Berryhill J.R.; 1984: *Wave-equation datuming before stack*. Geophys., **49**, 2064-2066.

Bevc D.; 1997: *Flooding the topography: wave-equation datuming of land data with rugged acquisition topography*. Geophys., **62**, 1558-1569.

Chamot-Rooke N., Rangin C. and Le Pichon X.; 2005: *DotMed "Deep offshore tectonics of the Mediterranean", a synthesis of deep marine data in the eastern Mediterranean*. Mém. Soc. Géol. France, **177**, 1-64.

Clément C., Him A., Charvis P., Sachpazi M. and Marnelis F.; 2000: *Seismic structure and the active Hellenic subduction in the Ionian islands*. Tectonophys., **329**, 141-156.

Feng L., Newman A.V., Farmer G.T., Psimoulis P. and Stiros S.C.; 2010: *Energetic rupture and post-seismic response of the 2008 Mw 6.4 Achaia-Elia Earthquake in northwestern Peloponnese, Greece: an indicator of an immature transform fault zone*. Geophys. J. Int., **183**, 103-110.

Fruehn J., Fliedner M. and White R.S.; 2001: *Case history: integrated wide-angle and near-vertical subbasalt study using large-aperture seismic data from the Faeroe - Shetland region*. Geophys., **66**, 1340-1348.

Fruehn J., Reston T., von Huene R. and Bialas J.; 2002: *Structure of the Mediterranean Ridge accretionary complex from seismic velocity information*. Mar. Geol., **186**, 43-58.

Gesret A., Laigle M., Diaz J., Sachpazi M. and Him A.; 2010: *The oceanic nature of the Africa slab subducted under Peloponnese: thin layer resolution from multiscale analysis of teleseismic P-to-S converted waves*. Geophys. J. Int., **183**, 833-849, doi:10.1111/j.1365-246X.2010.04738.x.

Him A., Sachpazi M., Siliqi R., McBride J., Marmelis F., Cernobori L. and the STREAMERS-PROFILES Group; 1996: *A traverse of the Ionian islands front with coincident normal incidence and wide-angle seismic*. Tectonophys., **264**, 35-49.

Jolivet L. and Brun J.P.; 2010: *Cenozoic geodynamic evolution of the Aegean*. Int. J. Earth Sci. (Geol. Rundsch.), **99**, 109-138, doi:10.1007/s00531-008-0366-4.

Jones K.A., Warner M., Le Meur D., Pascal G., Tay P.L. and IMERSE Working Group; 2002: *Wide-angle images of the Mediterranean Ridge backstop structure*. Mar. Geol., **186**, 145-166.

Kamberis E., Sotiropoulos S., Aximniotou O., Tsaila-Monopoli S. and Ioakim C.; 2000: *Late Cenozoic deformation of the Gavrovo and Ionian zones in NW Peloponnese (western Greece)*. Ann. Geof., **43**, 905-919.

Laigle M., Him A., Sachpazi M. and Clement C.; 2002: *Seismic coupling and structure of the Hellenic subduction zone in the Ionian island region*. Earth Planet. Sci. Lett., **200**, 243-253.

Lallemant S., Truffert C., Jolivet L., Henry P., Chamot-Rooke N. and de Voogd B.; 1994: *Spatial transition from compression to extension in the western Mediterranean Ridge accretionary complex*. Tectonophys., **234**, 33-52.

Le Pichon X., Lallemant S.J., Chamot-Rooke N., Lemeur D. and Pascal G.; 2002: *The Mediterranean Ridge backstop and the Hellenic nappes*. Mar. Geol., **186**, 111-125.

Liu Z.; 1993: *A Kirchhoff approach to seismic modeling and prestack depth migration*. Center for Wave Phenomena, Colorado School of Mines, Golden CO U.S.A., 22 pp.

Makris J.; 1978: *The crust and upper mantle of the Aegean region from deep seismic soundings*. Tectonophys., **46**, 269-284.

Papanikolaou D.J. and Royden L.H.; 2007: *Disruption of the Hellenic arc: Late Miocene extensional detachment faults and steep Pliocene - Quaternary normal faults - Or what happened at Corinth?* Tectonics, **26**, TC5003, doi:10.1029/2006TC002007.

Papoulia J., Makris J., Mascle J., Slejko D. and Yalçiner A.; 2014: *The EU SEAHELLARC project: aims and main results*. Boll. Geof. Teor. Appl., **55**, 341-348, doi: 10.4430/bgta0100.

Sachpazi M., Him A., Clément C., Haslinger F., Laigle M., Kissling E., Charvis P., Hello Y., Lépine J.C., Sapin M. and Ansorge J.; 2000: *Western Hellenic subduction and Cephalonia transform: local earthquakes and plate transport and strain*. Tectonophys., **319**, 301-319.

Slejko D., Santulin M. and Garcia J.; 2014: *Seismic hazard estimates for the area of Pylos and surrounding region (SW Peloponnese) for seismic and tsunami risk assessment*. Boll. Geof. Teor. Appl., **55**, 433-468, doi: 10.4430/bgta0090.

Sotiropoulos S., Kamberis E., Triantaphyllou M.V. and Doutsos T.; 2003: *Thrust sequences in the central part of the External Hellenides*. Geol. Mag., **140**, 661-668, doi:10.1017/S0016756803008367.

Suckale J., Rondenay S., Sachpazi M., Charalampakis M., Hosa A. and Royden L.H.; 2009: *High-resolution seismic imaging of the western Hellenic subduction zone using teleseismic scattered waves*. Geophys. J. Int., **178**, 775-791, doi:10.1111/j.1365-246X.2009.04170.x.

Truffert C., Chamot-Rooke N., Lallemant S., De Voogd B., Huchon P. and Le Pichon X.; 1993: *The crust of the western Mediterranean Ridge from deep seismic data and gravity modelling*. Geophys. J. Int., **114**, 360-372.

Underhill J.R.; 1989: *Late Cenozoic deformation of the Hellenides foreland western Greece*. Geol. Soc. Am. Bull., **101**, 613-634.

Van Hinsbergen D.J.J., Van der Meer D.G., Zachariasse W.J. and Meulenkamp J.E.; 2006: *Deformation of western Greece during Neogene clockwise rotation and collision with Apulia*. Int. J. Earth Sci., **95**, 463-490.

Yilmaz O.; 2001: *Seismic data analysis*. Investigations in Geophysics n. 10, vol. 1, Society of Exploration Geophysicists, Tulsa USA, 1000 pp.

Yilmaz O. and Lucas D.; 1986: *Prestack layer replacement*. Geophys., **51**, 1355-1369.

Wardell N., Camera L., Mascle J., Nicolich R., Marchi M. and Barison E.; 2014: *The structural framework of the Peloponnese continental margin from Zakynthos to Pylos from seismic reflection and morpho-bathymetric data*. Boll. Geof. Teor. Appl., **55**, 343-367, doi: 10.4430/bgta0087.

Wiggins J.W.; 1984: *Kirchhoff integral extrapolation and migration of nonplanar data*. Geophys., **49**, 1239-1248.

Corresponding author: Rinaldo Nicolich
Department of Civil and Environmental Engineering, University of Trieste
Piazzale Europa, 34100 Trieste, Italy
Phone: +30 040 5583478; fax: +39 040 5583497; e-mail: r.nicolich@units.it

Appendix
Wave equation datuming

Let us consider the wavefield *U(x,y,z;t)* propagating in a medium with a velocity *v(x,y,z)*; the scalar wave equation is:

$$\left[\frac{\partial^2}{\partial x^2}+\frac{\partial^2}{\partial y^2}+\frac{\partial^2}{\partial z^2}-\frac{1}{v^2(x,y,z)}\frac{\partial^2}{\partial t^2}\right]U(x,y,z;t)=0 \qquad \text{(A-1)}$$

A computationally efficient method of extrapolating a wavefield defined on a surface to points outside the surface is given by the integral equation approach to waves propagation problems.

Let us locate the receiver at the origin of coordinate system and the point diffractor at a generic location (*x,y,z*). We proceed with the Fourier direct transform in the time direction and the Green's function, which describes the wave propagation outwards from a point source with spherical symmetry, according to the Huygens' principle that every point on a wavefront can be regarded as the source of the subsequent wave. The mathematical details are summarized in Yilmaz (2001) and the solution in the time domain can be finally written as:

$$U(x,y,z,t) = \frac{1}{4\pi}\int_A \left\{ \frac{1}{r}\left[\frac{\partial U(\tau)}{\partial z}\right] + \frac{\cos\theta}{r^2}\left[U(\tau)\right] + \frac{\cos\theta}{vr}\left[\frac{\partial U(\tau)}{\partial t}\right] \right\} dA \,. \qquad \text{(A-2)}$$

The integration over the area *A* is done using the wavefield *U(x,y,z;t)* at the retarded time $\tau = t - r/v$; θ is the angle between *r* (the distance between the diffractor point and the point on the new datum) and the normal to the input datum; the first term depends on the vertical gradient of the wavefield; the second term is the near field decaying with $1/r^2$; the third term is the far field term.

Berryhill (1979) proposed an implementation of the Kirckhoff's integral solution to extrapolate seismic waves from one datum (indicated by the index *i*, Fig. A1) to another (indicated by the index *j*):

$$U_j(t) = \frac{1}{4\pi}\sum_i \Delta x_i \cos\theta_i \frac{t_i}{r_i}\left[U_i(\tau_i) * F_i\right] \,. \qquad \text{(A-3)}$$

The distance between the seismic traces U_i and U_j is r_i, τ_i corresponds to $t - r_i/v$, θ_i is the angle between r_i and the normal to the input datum, and Δx_i is the distance between adjacent trace locations. *F* is a filter operator, function of (τ_i, r_i, Δx_i, θ_i), to convolve with the trace to prevent distortions.

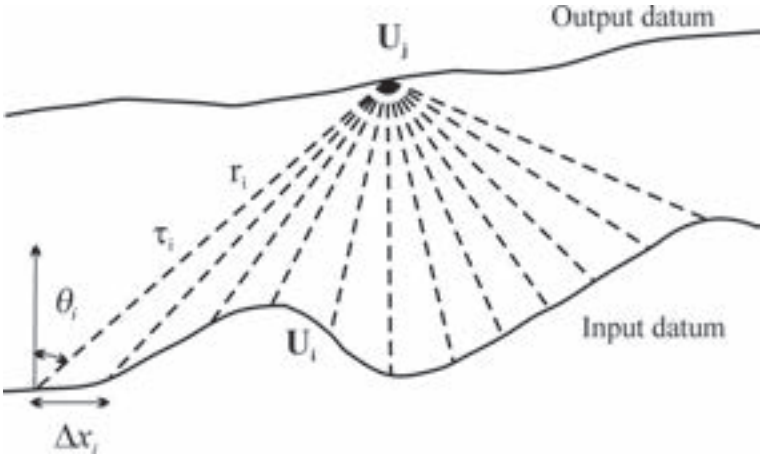

Fig. A1 - Schematic representation of the Kirchhoff upward and/or downward continuation from an input datum to the new output, corresponding to the implementation of Eq. (A-3).

In conclusion, Fig. A1 shows a schematic representation of the Kirchhoff upward continuation corresponding to implementation of Eq. (A-3): each input trace U_i is filtered, time-shifted according to $\tau_i = t\text{-}t_i$, scaled, and summed into output trace U_j.

A traveltime table between the input and the output datum, obtained by using velocity information is indispensable (Yilmaz and Lucas, 1986). In presence of complex structures and/or strong lateral velocity variation, the eikonal equation, which is a ray-theoretical approximation to the scalar wave equation, is adopted. Its solution represents wavefronts of constant phase. The wave is propagated from one wavefront to the next by raypaths, which are perpendicular to the wavefronts. In particular, the wavefield at a point on the output datum is computed using all the traces in the input gather. The output gather should be computed beyond the lateral extent of the input gather to prevent possible loss of steeply dipping events (Yilmaz, 2001).

Eq. (A-3) describes the upward continuation of upgoing waves and the downward continuation of downgoing waves-cases, in which the travelling wave encounters the input locations before the output location. If the travelling wave encounters the output location before the input location, it is necessary only to image a movie of the event run backwards to recover the situation previously considered. Thus, Eq. (A-3) permits the downward continuation of upgoing waves and viceversa, simply by time-reversing all input traces before processing and all output traces afterwards, that is the signs of the times t and t_i.